## ChemPhotoChem



European Chemical Societies Publishing



## **Accepted Article**

**Title:** 2D Covalent Organic Frameworks with Incorporated Mn Complex for Light Driven CO2 Reduction

Authors: Jier Huang, Denan Wang, Daniel Streater, and Yun Peng

This manuscript has been accepted after peer review and appears as an Accepted Article online prior to editing, proofing, and formal publication of the final Version of Record (VoR). This work is currently citable by using the Digital Object Identifier (DOI) given below. The VoR will be published online in Early View as soon as possible and may be different to this Accepted Article as a result of editing. Readers should obtain the VoR from the journal website shown below when it is published to ensure accuracy of information. The authors are responsible for the content of this Accepted Article.

To be cited as: ChemPhotoChem 10.1002/cptc.202100123

Link to VoR: https://doi.org/10.1002/cptc.202100123

WILEY-VCH

#### **ARTICLE**

# 2D Covalent Organic Frameworks with Incorporated Mn Complex for Light Driven CO<sub>2</sub> Reduction

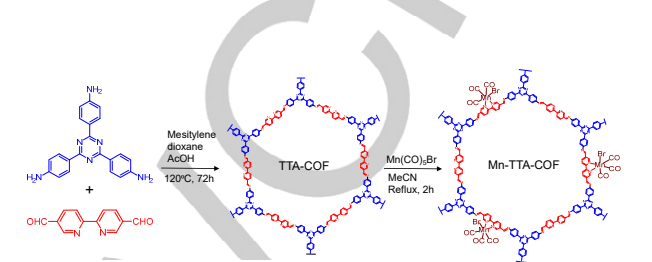
Denan Wang,[a] Daniel Streater,[a] Yun Peng,[a] and Jier Huang\*[a]

 Dr. D. Wang, D. Streater, Dr. Y. Peng, and Prof. J. Huang Department of Chemistry Marquette University Milwaukee, WI, 53201-1881 (USA) E-mail: jier.huang@marquette.edu

Abstract: Covalent organic frameworks (COFs) have emerged as a novel class of crystalline porous photocatalytic materials due to their unique properties such as large surface area, tunable porosity, and rigid structure. In this work, we report the direct incorporation of Mn CO2 molecular catalyst (MC) into COFs (Mn-TTA-COF) and the evaluation of its capability as photocatalyst for visible light driven CO2 reduction to form CO. We found that the photocatalytic activity of Mn-TTA-COF is quite low, which mainly results from the elimination of CO ligand in Mn MC upon light illumination, rendering its short duration in catalytic reaction. While this is a central concern to further use Mn-TTA-COF as CO<sub>2</sub> reduction catalyst, we found that the stability and efficiency of Mn MC is largely enhanced after being incorporated into COFs with respect to its homogeneous version, suggesting the capability of COFs as heterogeneous platform to incorporate MC and improve the catalytic performance of MC. Moreover, transient absorption spectroscopic studies show that the intramolecular charge transfer lifetime of Mn incorporated COF is longer than that in parent COF, which suggests that charge separation (CS) may occur from the parent COF to Mn moiety. These results together suggest the promise to use COFs as platform for creating next generation photocatalysts with built in photosensitizer and MC, which can facilitate CS and enhance the stability and efficiency of the incorporated MC.

#### Introduction

Artificial photosynthesis via photoreduction of CO<sub>2</sub> to form CO represents an important approach to simultaneously address the energy crisis and global warming issues. [1] The key challenge to achieve efficient photoreduction of CO2 arises from the high thermodynamic stability of CO2 and the competing hydrogen evolution reaction, rending high kinetic barrier and low selectivity for CO generation. Inspired from nature, one desirable approach to resolve these issues is to employ an appropriate photocatalytic system that integrates the photosensitizer (PS) and molecular catalyst (MC), which can not only significantly accelerate the kinetics but also provide active sites for CO<sub>2</sub> adsorption. [2] As such, various photocatalytic systems have been developed in the past decades, which include homogenous systems that incorporate molecular PS and MC, heterogeneous systems that combine solid state PS and catalyst, as well as hybrid systems that may integrate solid state/molecular PS and molecular/solid state catalyst. Despite many progresses, they all suffer from difficulties such as poor CO<sub>2</sub> adsorption, retarded charge separation (CS), as well as the fundamental insight on the structure-propertyfunction relationships.[1a, 3] It is therefore essential to develop novel photocatalytic materials that can further improve the efficiency and selectivity toward photoreduction of CO2.



**Scheme 1.** Synthetic scheme for the parent TTA-COF and Mn-TTA-COF.

Covalent organic frameworks (COFs) are a novel class of porous crystalline materials that are constructed from organic building units covalently linked into extended structure through the principles of reticular chemistry.[4] Due to their unique properties including high porosity, large surface area, structural flexibility, and chemical and thermal stability, COFs could offer a powerful platform for creating next generation photocatalysts. COFs are solely composed of light elements and held together by strong covalent bonds, which endows the potential to form robust and earth abundant photocatalytic materials. In addition, diverse options of organic ligands allow the inclusion of a large majority of available molecular functional units that have inherent light absorption and catalytic characteristics into their heterogeneous matrix, opening the possibility to integrate the beneficial features and overcome drawbacks of both homogeneous and heterogeneous catalysts. Motivated by the above-mentioned multi-fold advantages, researchers have demonstrated the capability of COFs for CO2 reduction through encapsulating various catalysts into COF structure, which include carbon dots.<sup>[5]</sup> semiconductor nanoparticles. [6] and transition metal molecular complexes such as Mn,[7] Cu,[8] Co,[9] Ni,[10] and Ir[11] complexes. Recently, we have also demonstrated that COFs with directly incorporated Re MC can efficiency catalyze CO<sub>2</sub> reduction to form CO with 98% selectivity upon visible light illumination. [12]

While these prior studies demonstrated the potential of COFs as platform for incorporating both PS and MC, it is necessary to further explore their capability as  $CO_2$  photocatalyst after embedding other MCs. In this work, we report the incorporation of Mn(CO)<sub>3</sub>(BPy)Br (BPy=2,2'-bipyridyl) MC into a TTA-COF based on 4,4',4"-(1,3,5-triazine-2,4,6-triyl) trianiline (TTA) and 2,2-bipyridyl-5,5'-dialdehyde (BPDA) to form Mn-TTA-COF (Scheme 1). We show that Mn-TTA-COF can catalyze  $CO_2$  reduction to form CO under visible light illumination with low efficiency due to the decomposition of Mn moiety through the elimination of CO ligand. Although the poor stability of Mn moiety decreases the optimism to further use it as  $CO_2$  reduction catalyst, its stability

#### **ARTICLE**

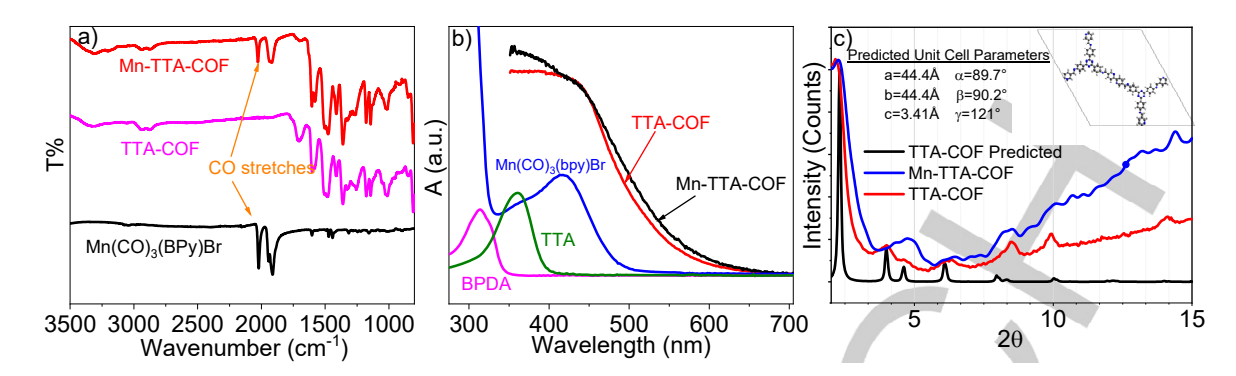


Figure 1. (a) FT-IR spectra of TTA-COF, Mn-TTA-COF, and Mn(CO)<sub>3</sub>(BPy)Br model complex. (b) Diffuse reflectance UV-visible spectra of TTA-COF, Mn-TTA-COF, Mn(CO)<sub>3</sub>(BPy)Br model complex, TTA monomer, and BPDA monomer. (c) Powder XRD patterns of TTA-COF, Mn-TTA-COF, and predicted pattern of TTA-COF. The inset shows the unit cell and unit cell parameters that were obtained for TTA-COF structure optimization by DFTB.

and efficiency in Mn-TTA-COF is much higher than its homogeneous counterpart. These results confirm our hypothesis that COF can serve as a powerful platform to enhance the stability and activity of the homogeneous system after being incorporated into a heterogeneous matrix. In addition, the excited state lifetime

of Mn-TTA-COF measured by transient absorption (TA) spectroscopy is longer than that of TTA-COF, which suggests that CS may occur from the parent TTA-COF to Mn moiety in Mn-TTA-COF.

#### **Results and Discussion**

#### Synthesis and Characterization of Mn-TTA-COF.

2D parent TTA-COF is synthesized by reacting TTA with BPDA in mixed dioxane/mesitylene as solvent and acetic acid as condensation reaction catalyst. [13] Mn moiety (Mn(CO)\_3(BPy)Br) which is expected to act as CO\_2 reduction catalyst is then incorporated to the parent TTA-COF by refluxing the TTA-COF and manganese pentacarbonyl bromide (Mn(CO)\_5Br) in acetonitrile for 2 hours under dark, which results into the formation of Mn-TTA-COF (Scheme 1). The details of synthetic procedure are provided in the experimental session.

The formation of the parent TTA-COF and Mn-incorporated Mn-TTA-COF is well supported by their FT-IR spectra. As shown in Figure S1, the FTIR spectrum of TTA-COF shows a characteristic -C=N stretch at 1629 cm<sup>-1</sup>, which is accompanied by the reduced intensity of the aldehyde C=O stretch (1698 cm<sup>-1</sup>) in BPDA and N-H stretch (3212 and 3309 cm<sup>-1</sup>) in TTA, supporting the conversion of the monomers via the condensation reaction to form TTA-COF. The FT-IR spectrum of Mn-TTA-COF shows intense CO stretch at 1925, 1932 and 2022 cm<sup>-1</sup>, which are consistent with the CO stretch of model complex Mn(CO)<sub>3</sub>(BPy)Br (Figure 1a), suggesting the successful incorporation of Mn moiety to TTA-COF. The formation of parent TTA-COF and Mn-TTA-COF is further supported by their diffuse reflectance UV-Visible (DR-UV-Vis) spectra, where an additional absorption in visible region, corresponding to the intramolecular charge transfer (ICT) band, is observed with respect to their corresponding monomers (Figure 1b). Slight red shift of ICT band (~10 nm) is observed in Mn-TTA-COF with respect to TTA-COF, which is similar to previously reported Re complex incorporated COFs and can be attributed to the vibronic broadening and/or enhanced delocalization due to the chelation of Mn(CO)<sub>3</sub>(BPy)Br. [12, 14] The crystallinity nature of these COFs is evaluated using powder Xray diffraction (PXRD). As shown in Figure 1c, the PXRD patterns of Mn-TTA-COF show multiple diffraction peaks that agree well with those in parent TTA-COF, suggesting the retain of crystalline nature upon the incorporation of Mn MC. However, the crystallinity of Mn-TTA-COF becomes slightly worse compared to that of TTA-COF. This might result from the complexation reaction between the TTA-COF and Mn(CO)<sub>5</sub>Br molecules, where Mn(CO)<sub>3</sub>(BPy)Br moiety that is incorporated to TTA-COF is randomly distributed in the cavity of TTA-COF, resulting into more disorder structure and slightly impact the packing of COF. The lattice model of TTA-COF simulated by Materials Studio software 8.0[15] yields the most probable structure of TTA-COF with AA stacking mode. The PXRD patterns resulted from the Pawley refinement of the simulated structure agree well with the experimental PXRD data (Figure 1c), suggesting the validity of our computational model. The composition of Mn element in the Mn-TTA-COF, measured by the inductively coupled plasma mass spectrometry (ICP-MS), is found to be 2.8% (weight percentage), which corresponds to 0.71 Mn per hexagon unit.

#### Photocatalytic performance

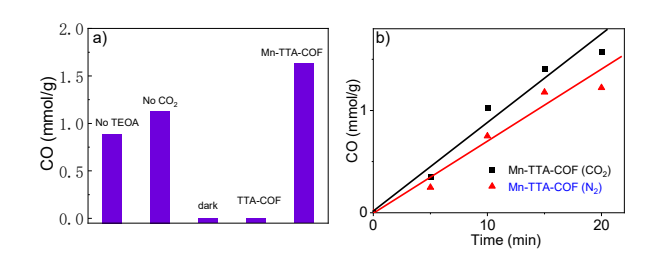


**Figure 2.** a) Control experiments by selectively omitting one component in the photocatalytic system. B) Time profile of Mn-TTA-COF for CO generation.

#### **ARTICLE**

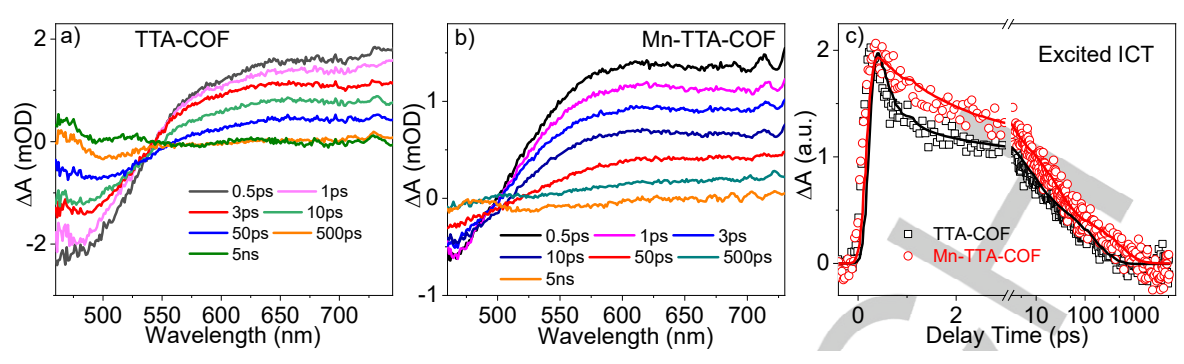


Figure 3. Transient absorption spectra of TTA-COF (a) and Mn-TTA-COF (b) following 400 nm excitation. (c) The comparison of kinetic traces of excited ICT at 650 nm between TTA-COF and Mn-TTA-COF. The open symbols are expereimental data and the solid lines are fitting results.

With good amount of Mn-TTA-COF on hand, which was characterized by FT-IR, DR-UV-Vis spectra and XRD, we proceed to investigate their photocatalytic activity for CO2 reduction in the presence of triethanolamine (TEOA) as the sacrificial donor, acetonitrile as solvent, and Xe lamp (cutoff wavelength = 420 nm) as light source. After 1 hour irradiation, the system can produce ~1.7 mmol CO/g of Mn-TTA-COF (Figure 2a) and no other products are detected in the liquid phase. Control experiments by omitting one component in the system shows that in the absence of Mn moiety or light illumination, no CO was detected, suggesting that these two components are essential for CO production (Figure 2a). Surprisingly, under N2 atmosphere without the presence of CO<sub>2</sub>, Mn-TTA-COF can generate CO with 1.2 mmol CO/g catalyst (Figure 2a), suggesting that the produced CO in N<sub>2</sub> atmosphere is possibly a result of decomposition of Mn moiety during photocatalysis. This is further supported by the FT-IR spectrum of Mn-TTA-COF collected after photocatalysis, where the peaks corresponding to CO-stretch in Mn moiety vanished (Figure S1). However, compared to that in CO<sub>2</sub> atmosphere, less CO is produced under N<sub>2</sub>, suggesting that photocatalytic reduction of CO<sub>2</sub> to form CO also occurs and contributes to the overall amount of CO produced. This is further supported by running the catalytic reaction under <sup>13</sup>CO<sub>2</sub> atmosphere, where gas chromatography mass spectrometry (GC-MS, Figure S2) detects both  $^{13}$ CO (m/z = 29) and  $^{12}$ CO (m/z = 28). The generated  $^{13}$ CO cannot come from the decomposition of <sup>13</sup>CO<sub>2</sub> gas because the control experiment by running pure <sup>13</sup>CO<sub>2</sub> through GC-MS does not generate <sup>13</sup>CO. These results together suggest that the generated CO comes from both CO2 through photocatalytic reduction and the decomposition of Mn(CO)<sub>3</sub>(BPy)Br in Mn-TTA-COF.

To gain more insight on the stability and efficiency of Mn-TTA-COF for  $CO_2$  reduction, the time profile of CO generation is collected under both  $N_2$  and  $CO_2$  atmosphere. As shown in Figure 2b, the system can produce CO steadily for  $\sim$  15 minutes upon the irradiation with Xe lamp under both conditions. However, the amount of CO generated in  $CO_2$  are obviously higher than in  $N_2$  atmosphere, which is consistent with the results discussed above, suggesting that Mn-TTA-COF can catalyze  $CO_2$  reduction to form CO but suffers from quick decomposition of the Mn moiety via elimination of CO ligand. In addition, the control system using model complex Mn(CO)<sub>3</sub>(BPy)Br as catalyst shows that the model complex can also generate CO (turn over number (TON) = 0.81 vs. 3.34 for Mn-TTA-COF) in  $CO_2$  atmosphere but only last 5 minutes, after which CO production stops. These results together

suggest that due to poor stability of  $Mn(CO)_3(BPy)Br$  under light, incorporation this MC to TTA-COF is not an optimal choice for the design of COF based photocatalysts for  $CO_2$  reduction. However, both the stability and efficiency of  $Mn(CO)_3(BPy)Br$  in Mn-TTA-COF appear to be higher than its homogenous version, which implies the promise of using COFs as platform to construct COF photocatalytic materials with built in PS and MC when more stable MCs other than  $Mn(CO)_3(BPy)Br$  were chosen.

To gain insight of photophysical properties of Mn-TTA-COF, which is the key parameter that determines its application for photocatalysis, we examined its excited state dynamics using femtosecond transient absorption (TA) spectroscopy. Figure 3a shows the TA spectra of TTA-COF following 400 nm excitation. Immediately following the excitation, we observed a negative feature at < 500 nm and a broad absorption feature at > 500 nm, which can be assigned to the stimulated emission/ground state bleach and excited ICT absorption, respectively, consistent with our previous findings.[13] While the TA spectra of Mn-TTA-COF also show the similar two main spectral features (Figure 3b), the isosbestic point of Mn-TTA-COF shifts to blue compared to that of TTA-COF, suggesting incorporation of Mn moiety to TTA-COF has impact on its excited state properties. The comparison of the kinetic traces at 650 nm corresponding to excited ICT shows that Mn-TTA-COF (108.6 ps) has a longer lifetime than that in TTA-COF (33.2 ps) (Table S1). These results, consistent with previously reported Re molecular complex incorporated COFs, suggest that charge transfer occurs from the parent TTA-COF to Mn moiety, resulting into a more separated CS state than that in TTA-COF. Note that the presence of charge transfer from the parent TTA-COF to Mn moiety is essential to reduce Mn moiety such that the latter can be activated to catalyze CO2 reduction reaction, which is likely responsible for the observed production of CO.

#### Conclusion

In summary, we report the synthesis, the photocatalytic performance, and photophysical studies on TTA-COF with incorporated Mn(CO) $_3$ (BPy)Br CO $_2$  reduction catalyst. We show that Mn(CO) $_3$ (BPy)Br can be successfully incorporated to parent TTA-COF through the coordination of Mn to bipyridyl ligand on TTA-COF to form Mn-TTA-COF. In the presence of TEOA as sacrificial donor, acetonitrile as solvent, Xe lamp as light source, Mn-TTA-COF can reduce CO $_2$  to form CO. However, the system

#### **ARTICLE**

can also generate CO in the absence of CO<sub>2</sub> (N<sub>2</sub> atmosphere) but with less CO product, suggesting that both the decomposition of Mn moiety and photoreduction of CO2 to form CO contribute to the produced CO. The decomposition of Mn moiety is believed to occur through elimination of CO ligand as supported by the varnishing of CO stretch in FTIR spectra of Mn-TTA-COF after catalysis. While the poor stability of Mn moiety in COF implies the challenge to use this system for photocatalysis, it was found that the duration of Mn(CO)<sub>3</sub>(BPy)Br embedded in COFs is much longer and TON is higher than its homogeneous version. In addition, transient absorption spectroscopic studies revealed that the lifetime of the ICT state is more than 3 times longer in Mn-TTA-COF than TTA-COF, which suggests that CS occurs from the parent TTA-COF to Mn moiety. These results together suggest although Mn(CO)<sub>3</sub>(BPy)Br may not be a good candidate as molecular catalyst, it is promising to develop highly robust COF photocatalysts by incorporating more robust molecular catalysts into its heterogeneous framework, which is expected to facilitate charge separation and enhance both stability and efficiency.

#### **Experimental Section**

#### Synthesis.

**Materials:** 2,2'-bipyridyl-5,5'-dialdehyde (97%, Amadis Chemical), Manganese pentacarbonyl bromide (98%, Sigma-Aldrich), Mesitylene (99%, Acros Organics), 1,4-dioxane (anhydrous, EMD Millipore Corporation), glacial acetic acid (ACS reagent, Acros Organics). 4,4',4"-(1,3,5-triazine-2,4,6-triyl)trianiline (TTA) is synthesized following the literature report.[16]

Synthesis of model complex Mn(BPy)(CO)<sub>3</sub>Br: Mn(CO)<sub>5</sub>Br (0.199 g, 0.72 mmol) and 2,2'-bipyridyl (0.111 g, 0.71 mmol) was dissolved in 30 mL of hot diethyl ether. The mixture was stirred and refluxed for 3 hours to get yellow powder product by precipitation. The obtained power product was further washed by diethyl ether and dried under vacuum. <sup>1</sup>H NMR (acetonitrile-d<sub>3</sub>)  $\delta$  9.24 (d, J = 5.1 Hz, 2H), 8.36 (d, J = 8.1 Hz, 2H), 8.13 (t, J = 7.5 Hz, 2H), 7.63 (t, J = 6.1 Hz, 2H).

**Synthesis of TTA-COF:**<sup>[13]</sup> In a 10 mL pressure tube, 4,4',4"-(1,3,5-triazine-2,4,6-triyl)trianiline (TTA) (92 mg) and 2,2-bipyridyl-5,5-dialdehyde (BPDA) (82.68 mg) were dispersed in a mixture of mesitylene (5.1 mL), dioxane (0.9 mL) and glacial acetic acid (0.2 mL). After degassing, the tube was sealed and heated to 120 °C for 3 days. The resulting solid was collected by centrifugation and washed with THF repeatedly to remove the trapped guest molecules. The powder was then dried under vacuum to produce TTA-COF in an isolated yield of 65%.

Synthesis of Mn-TTA-COF: TTA-COF (50 mg) and Mn(CO) $_5$ Br (20 mg, 0.073 mmol) were dispersed in 10 mL acetonitrile under argon atmosphere. The mixture was refluxed for 30 mins under stirring and excluding light (covered with aluminum foil). The orange products were filtered and washed with methanol for 3 times. The Mn content in Mn-COF is determined by ICP-MS as 2.8 wt%.

#### General characterization.

SEM was performed with a JEOL JSM-6510LV operating in the secondary electron mode. Diffuse reflectance UV-Visible absorption spectra were taken using an Agilent 8453 spectrometer. Infrared (IR) spectra of solid samples were measured with a Thermo Scientific Nicolet iS5 FTIR spectrometer equipped with the iD3 attenuated total reflectance accessory. PXRD data were collected by using Rigaku Miniflex II XRD

diffractometer with Cu K $\alpha$  radiation. <sup>1</sup>H NMR spectra were collected at room temperature with a Varian 400 MHz spectrometer. The amount of CO generated was quantified using Agilent 490 micro gas chromatograph (5Å molecular sieve column). To make COF films, 1 mg COF was mixed with 0.5 mL Nafion (5% w/w in water and 1-propanol). The mixture was sonicated for 2 h and then dispersed evenly on piranha-etched glass. The films were dried in the air. Mass spectra were recorded from Shimadzu GCMS-QP2010 SE spectrometer with an 19091P-MS4E column (30 m, 0.32 mm, 12  $\mu$ m).

#### **Computational Structure Optimization**

Periodic self-consistent charge density functional tight-binding (SCC-DFTB) implemented in DFTB+[18] (version 19.1) was used to optimize periodic structures of TTA-COF. The unit cell was obtained from a reference<sup>[19]</sup> and optimized with parameters from 3ob-3-1ref Slater-Koster files<sup>[20]</sup> BJ damped<sup>[21]</sup> D3 dispersion<sup>[22]</sup> (a1=0.746, a2=4.191, s6=1.0, s8=3.209), three-body interactions, an additional H-H repulsion correction<sup>[23]</sup>, finite difference differentiation delta parameter of 1.22x10<sup>-4</sup>, error in the SCC calculation minimized by Broyden density mixer parameter of 0.2, inverse Jacobi weight of 1x10<sup>-2</sup>, and Ewald tolerance for boundary conditions of 1x10<sup>-9</sup> until no force over 1x10<sup>-4</sup> was acting on any atom, and no force over 1x10<sup>-4</sup> was acting on the lattice vectors. The predicted PXRD pattern was generated in Mercury 2.0 with the FWHM value set to 0.5.

#### Photocatalytic CO<sub>2</sub> reduction.

Samples for CO $_2$  reduction were prepared in 11 mL septum-sealed glass vials. Each sample was made up to a volume of 4 mL, including 0.9 mg of Mn-TTA-COF, 3.8 mL of CH $_3$ CN, and 0.2 mL of triethanolamine (TEOA). The mixture was purged with CO $_2$  for 20 mins before irradiation by a 300W Xe lamp (420 nm cut off). The mixture was kept stirring during photocatalytic reaction. The amount of CO product was quantified using Agilent 490 micro gas chromatograph (5 Å molecular sieve column) by analysing 200  $\mu$ L of the headspace gas. For the  $^{13}$ C isotope experiment, the photocatalytic reaction was carried out under  $^{13}$ CO $_2$  atmosphere for 30 mins, after which the headspace gas was injected into GC-MS for analysis.

#### Femtosecond Transient Absorption (TA) Spectroscopy.

The femtosecond TA spectroscopy is based on a regenerative amplified Ti-Sapphire laser system (Solstice, 800 nm, < 100 fs FWHM, 3.5 mJ/pulse, 1 kHz repetition rate). The tunable pump (235-1100 nm), chopped at 500 Hz, is generated in TOPAS from 75% of the split output from the Ti-Sapphire laser. The other 25% generated tunable UV-visible probe pulses by while light generation in a Sapphire window (450-750 nm) on a translation stage. Helios ultrafast spectrometer (Ultrafast Systems LLC) was used to collect the spectra. The film samples were continuously translated to avoid heating and permanent degradation. The pump power (400 nm) at the sample is 0.3 mW.

#### Acknowledgements

This research is supported by the U.S. Department of Energy, Office of Science, Office of Basic Energy Sciences, under Award No. DE-SC0020122.

**Keywords:** Covalent Organic Frameworks • Photocatalytic CO<sub>2</sub> reduction • Mn Molecular Catalysts • Transient Absorption Spectroscopy • Excited State Dynamics

[1] a) T. Inoue, A. Fujishima, S. Konishi and K. Honda, *Nature* **1979**, 277, 637-638; b) D. M. D'Alessandro, B. Smit and J. R. Long, *Angewandte Chemie-International Edition* **2010**, 49, 6058-6082; c) A. M. Appel, J. E. Bercaw, A. B. Bocarsly, H. Dobbek, D. L. DuBois,

#### WILEY-VCH

#### **ARTICLE**

M. Dupuis, J. G. Ferry, E. Fujita, R. Hille, P. J. A. Kenis, C. A. Kerfeld, R. H. Morris, C. H. F. Peden, A. R. Portis, S. W. Ragsdale, T. B. Rauchfuss, J. N. H. Reek, L. C. Seefeldt, R. K. Thauer and G. L. Waldrop, *Chemical Reviews* **2013**, *113*, 6621-6658. [2] a) V. S. Thoi, N. Kornienko, C. G. Margarit, P. D. Yang and C. J. Chang, *Journal of the American Chemical Society* **2013**, *135*, 14413-14424; b) E. E. Barton, D. M. Rampulla and A. B. Bocarsly, *Journal of the American Chemical Society* **2008**, *130*, 6342-+; c) J. M. Smieja, E. E. Benson, B. Kumar, K. A. Grice, C. S. Seu, A. J. M. Miller, J. M. Mayer and C. P. Kubiak, *Proceedings of the National Academy of Sciences of the United States of America* **2012**, *109*, 15646-15650.

[3] a) J. L. White, M. F. Baruch, J. E. Pander, Y. Hu, I. C. Fortmeyer, J. E. Park, T. Zhang, K. Liao, J. Gu, Y. Yan, T. W. Shaw, E. Abelev and A. B. Bocarsly, *Chemical Reviews* **2015**, *115*, 12888-12935; b) S. B. Wang, W. S. Yao, J. L. Lin, Z. X. Ding and X. C. Wang, *Angewandte Chemie-International Edition* **2014**, *53*, 1034-1038; c) S. B. Wang and X. C. Wang, *Angewandte Chemie-International Edition* **2016**, *55*, 2308-2320.

[4] a) C. S. Diercks and O. M. Yaghi, *Science* **2017**, *355*; b) S. Kandambeth, K. Dey and R. Banerjee, *Journal of the American Chemical Society* **2019**, *141*, 1807-1822; c) D. D. Medina, T. Sick and T. Bein, *Advanced Energy Materials* **2017**, *7*; d) E. Q. Jin, M. Asada, Q. Xu, S. Dalapati, M. A. Addicoat, M. A. Brady, H. Xu, T. Nakamura, T. Heine, Q. H. Chen and D. L. Jiang, *Science* **2017**, *357*, 673-676; e) L. Garzon-Tovar, S. Rodriguez-Hermida, I. Imaz and D. Maspoch, *Journal of the American Chemical Society* **2017**, *139*, 897-903; f) H. Y. Kang, H. Wang, J. Huang, Y. J. Wang, D. Y. Li, C. D. Diao, W. Zhu, Y. Tang, Y. Wang, X. Fan, J. Zeng, L. L. Xu, L. N. Sha, H. Q. Zhang and Y. H. Zhou, *Plos One* **2016**, *11*; g) N. Keller, D. Bessinger, S. Reuter, M. Calik, L. Ascherl, F. C. Hanusch, F. Auras and T. Bein, *Journal of the American Chemical Society* **2017**, *139*, 8194-8199; h) D. N. Bunck and W. R. Dichtel, *Journal of the American Chemical Society* **2013**, *135*, 14952-14955; i) R. P. Bisbey and W. R. Dichtel, *Acs Central Science* **2017**, *3*, 533-543. [5] H. Zhong, R. Sa, H. Lv, S. Yang, D. Yuan, X. Wang and R. Wang, *Adv. Funct. Mater.* **2020**, *30*, 2002654.

[6] K. Guo, X. Zhu, L. Peng, Y. Fu, R. Ma, X. Lu, F. Zhang, W. Zhu and M. Fan, *Chem. Eng. J. (Amsterdam, Neth.)* **2021**, *405*, 127011. [7] G. C. Dubed Bandomo, S. S. Mondal, F. Franco, A. Bucci, V. Martin-Diaconescu, M. A. Ortuño, P. H. van Langevelde, A. Shafir, N. López and J. Lloret-Fillol, *ACS Catalysis* **2021**, *11*, 7210-7222. [8] B. Wang, F. Yang, Y. Dong, Y. Cao, J. Wang, B. Yang, Y. Wei, W. Wan, J. Chen and H. Jing, *Chem. Eng. J. (Amsterdam, Neth.)* **2020**, *396*, 125255.

[9] a) X. Wang, Z. Fu, L. Zheng, C. Zhao, X. Wang, S. Y. Chong, F. McBride, R. Raval, M. Bilton, L. Liu, X. Wu, L. Chen, R. S. Sprick and A. I. Cooper, *Chem. Mater.* **2020**, *32*, 9107-9114; b) C. Wang, X.-M. Liu, M. Zhang, Y. Geng, L. Zhao, Y.-G. Li and Z.-M. Su, *ACS Sustainable Chem. Eng.* **2019**, 7, 14102-14110.

[10] a) N. Xu, X. Qin, H. Ke, Y. Diao, Z. Xu and X. Zhu, *Dalton Trans* **2020**, *49*, 15587-15591; b) W. Zhong, R. Sa, L. Li, Y. He, L. Li, J. Bi, Z. Zhuang, Y. Yu and Z. Zou, *J. Am. Chem. Soc.* **2019**, *141*, 7615-7621.

[11] S.-Q. You, J. Zhou, M.-M. Chen, C.-Y. Sun, X.-J. Qi, A. Yousaf, X.-L. Wang and Z.-M. Su, *J. Catal.* **2020**, 392, 49-55.

[12] S. Z. Yang, W. H. Hu, X. Zhang, P. L. He, B. Pattengale, C. M. Liu, M. Cendejas, I. Hermans, X. Y. Zhang, J. Zhang and J. E. Huang, *Journal of the American Chemical Society* **2018**, *140*, 14614-14618

[13] S. Yang, W. Hu, X. Zhang, P. He, B. Pattengale, C. Liu, M. Cendejas, I. Hermans, X. Zhang, J. Zhang and J. Huang, *J Am Chem Soc* **2018**, *140*, 14614-14618.

[14] X. X. Qiao, Q. Q. Li, R. N. Schaugaard, B. W. Noffke, Y. J. Liu, D. P. Li, L. Liu, K. Raghavachari and L. S. Li, *Journal of the American Chemical Society* 2017, 139, 3934-3937.

[15] S. Y. Ding, J. Gao, Q. Wang, Y. Zhang, W. G. Song, C. Y. Su and W. Wang, *Journal of the American Chemical Society* **2011**, *133*, 19816-19822.

[16] R. Gomes, P. Bhanja and A. Bhaumik, *Chemical Communications* **2015**, *51*, 10050-10053.

[17] M. Bourrez, F. Molton, S. Chardon-Noblat and A. Deronzier, Angewandte Chemie-International Edition 2011, 50, 9903-9906.
[18] B. Aradi, B. Hourahine and T. Frauenheim, Journal of Physical Chemistry A 2007, 111, 5678-5684.

[19] R. Mercado, R. S. Fu, A. V. Yakutovich, L. Talirz, M. Haranczyk and B. Smit, *Chemistry of Materials* **2018**, *30*, 5069-5086.

[20] M. Gaus, A. Goez and M. Elstner, *Journal of Chemical Theory and Computation* **2013**, 9, 338-354.

[21] E. R. Johnson and A. D. Becke, *Journal of Chemical Physics* **2005**, *123*.

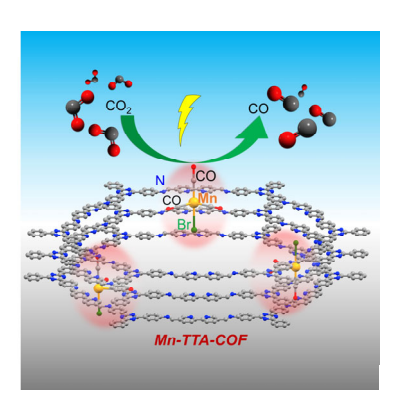
[22] S. Grimme, J. Antony, S. Ehrlich and H. Krieg, *Journal of Chemical Physics* **2010**, *132*.

[23] J. Rezac and P. Hobza, *Journal of Chemical Theory and Computation* **2012**, *8*, 141-151.

WILEY-VCH

### **ARTICLE**

#### **Entry for the Table of Contents**



Mn(CO<sub>3</sub>)(BPy)Br molecular complex is incorporated into TTA-COF (Mn-TTA-COF), which can catalyze visible light driven CO<sub>2</sub> reduction to form CO with significantly enhanced stability and efficiency with respect to its homogenous version. Transient absorption spectroscopic studies demonstrate charge transfer from the parent TTA-COF to Mn moiety.

